Probing the Mechanism of Insulin Fibril Formation with Insulin Mutants†

Liza Nielsen,‡ Sven Frokjaer,§ Jens Brange, Vladimir N. Uversky,‡ and Anthony L. Fink*,‡

University of California−Santa Cruz, Department of Chemistry and Biochemistry, Santa Cruz, California 95064, and Department of Pharmaceutics, The Royal Danish School of Pharmacy, 2100 Copenhagen, Denmark, Biologics Development - Pharmaceutics, Novo Nordisk A/S, 2880 Bagsvaerd, Denmark

Received March 26, 2001; Revised Manuscript Received May 21, 2001

ABSTRACT: The molecular basis of insulin fibril formation was investigated by studying the structural properties and kinetics of fibril formation of 20 different human insulin mutants at both low pH (conditions favoring monomer/dimer) and at pH 7.4 (conditions favoring tetramer/hexamer). Small-angle X-ray scattering showed insulin to be monomeric in 20% acetic acid, 0.1 M NaCl, pH 2. The secondary structure of the mutants was assessed using far-UV circular dichroism, and the tertiary structure was determined using near-UV circular dichroism, quenching of intrinsic fluorescence by acrylamide and interactions with the hydrophobic probe 1-anilino-8-naphthalene-sulfonic acid (ANS). The kinetics of fibril formation were monitored with the fluorescent dye, Thioflavin T. The results indicate that the monomer is the state from which fibrils arise, thus under some conditions dissociation of hexamers may be rate limiting or partially rate limiting. The insulin mutants were found to retain substantial nativelike secondary and tertiary structure under all conditions studied. The results suggest that fibril formation of the insulin mutants is controlled by specific molecular interactions that are sensitive to variations in the primary structure. The observed effects of several mutations on the rate of fibril formation are inconsistent with a previously suggested model for fibrillation [Brange, J., Whittingham, J., Edwards, D., Youshang, Z., Wollmer, A., Brandenburg, D., Dodson, G., and Finch, J. (1997) *Curr. Sci. 72,* 470−476]. Two surfaces on the insulin monomer are identified as potential interacting sites in insulin fibrils, one consisting of the residues B10, B16, and B17 and the other consisting of at least the residues A8 and B25. The marked increase in the lag time for fibril formation with mutations to more polar residues, as well as mutations to charged residues, demonstrates the importance of both hydrophobic and electrostatic interactions in the initial stages of fibrillation. A model for insulin fibril formation is proposed in which the formation of a partially folded intermediate is the precursor for associated species on the pathway to fibril formation.

Insulin is a small protein hormone that is crucial for the control of glucose metabolism and in diabetes treatment. It is composed of two polypeptide chains, the A-chain (21 residues) and the B-chain (30 residues) linked together by two disulfide bonds (*1*, *2*). In solution, insulin exists as an equilibrium mixture of monomers, dimers, tetramers, hexamers, and possibly higher associated states, depending on concentration, pH, metal ions, ionic strength, and solvent composition (*3*). The physiologically predominant storage form of insulin is a zinc-coordinated hexamer, formed by the association of three dimers, and stabilized by two to four zinc ions. Zinc-free insulin is a dimer at low protein concentrations over the pH 2−8 range, shifting to a tetramer at protein concentrations above 1.5 mg/mL (*4*). Upon exposure to elevated temperatures, low pH, organic solvents and agitation, insulin is susceptible to fibril formation (*5*, *6*). Although several studies have attempted to identify the specific residues involved in the interactions between units in fibrillar insulin, the molecular mechanism of insulin fibril formation is still not fully understood.

Recently, a model for the organization of insulin molecules in the insulin fibril has been proposed based on the crystal structure of the monomeric insulin mutant, des-pentapeptide (B26−30) insulin (DPI)[1] (*7*). Two sets of hydrophobic interactions in the fibril model were suggested. One set of contacts involved the aliphatic residues, Ile^{A2}, Val^{A3}, Leu^{B11}, and Leu^{B15}, exposed when the B-chain C-terminal is displaced, in contact with a hydrophobic surface consisting of Leu^{A13}, Leu^{B6}, Ala^{B14}, Leu^{B17}, and Val^{B18}, normally buried when three insulin dimers form a hexamer (dimer−dimer interface; in the following referred to as hexamer interfaces). The second set of contacts in the fibril model was considered to be an antiparallel β-sheet structure between the residues B1 and B5, running perpendicular to the length axis of the fibrils. The β-sheet was thought to be a favorable contact through which bundles of fibrils may develop from individual fibrils (*7*).

† This research was supported by the Academy of Technical Sciences (ATV) in Denmark and a grant from the University of California BioSTAR program.

* To whom correspondence should be addressed. E-mail: enzyme@cats.ucsc.edu. Phone: (831) 459-2744. Fax: (831) 459-2935.

‡ University of California.

§ Department of Pharmaceutics. Current affiliation: Brange Consult, Kroyersvej 22C, 2930 Klampenborg, Denmark.

[1] Abbreviations: DPI, des-pentapeptide (B26−30) insulin; CD, circular dichroism; ThT, Thioflavin T; ANS, 1-anilino-8-naphthalene-sulfonic acid; SAXS, small-angle X-ray scattering; R_g, radius of gyration; TEM, transmission electron microscopy.

10.1021/bi0105983 CCC: $20.00
Published on Web 06/19/2001

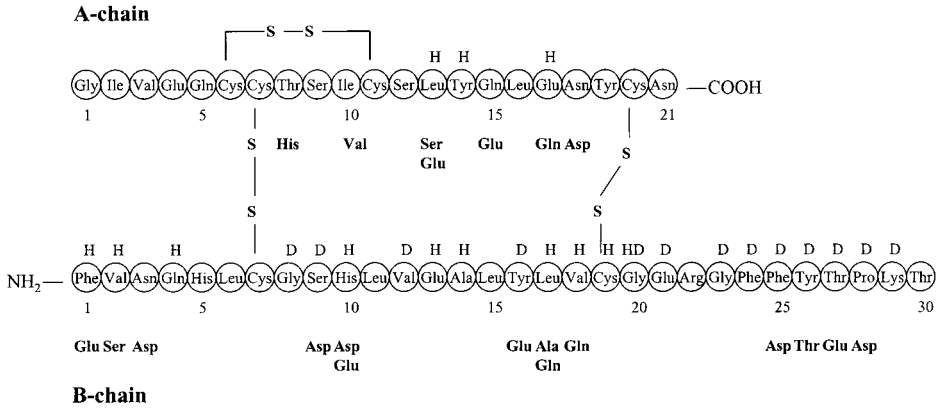

FIGURE 1: Primary structure of human insulin. The superscripts indicate the amino acid residues involved in association of insulin into dimers (D) and hexamers (H). Sites and type of mutation in different insulin mutants are shown below the respective residues (for composition of individual mutants see Table 2).

On the basis of the model of insulin fibrils, it was predicted that substitution of the nonpolar residues Leu^{A13}, Ala^{B14}, Leu^{B17}, and Val^{B18} by residues with polar side chains would impair the nonpolar packing made by these residues along the fiber axis making them less prone to form fibrils (*8*). It was also predicted that removal of the B-chain N-terminal residues would prevent the assembly of fibrils into bundles of fibrils (lateral aggregation).

To investigate the molecular interactions in insulin fibrils, a variety of human insulin mutants were selected with one or more mutations (Figure 1). The mutants included mutations in the two predicted hydrophobic interacting sites as well as in residues involved in either the dimer or hexamer interfaces. Bovine insulin was also included, as it is known to be much more prone to form fibrils than human insulin (*9*). Bovine insulin differs from human in three positions. It contains Ala in place of Thr at A8, Val in place of Ile at A10, and Ala in place of Thr at B30. Two mutants with substitutions in A8 and A10, respectively, were chosen in an attempt to identify the amino acid residues responsible for the faster fibrillation of bovine compared to human insulin.

Several observations suggest that insulin fibril formation proceeds through the monomer. First of all, the ease with which monomeric and truncated insulin mutants form fibrils strongly indicate that fibril formation requires an interaction between monomers (*8*). The increasing tendency for insulin fibril formation with decreasing pH, which results in an increased population of monomers and dimers, also supports the idea that fibril formation starts from the monomer (*9*, *10*). If monomerization of oligomeric insulin is a prerequisite for fibril formation, the process should be very sensitive to variations in the association state of the different mutants. At neutral pH, the association states of the mutants range from monomeric to tetrameric (*11*). Wild-type insulin forms hexamers at neutral pH in the presence of zinc. Fibril formation of the mutants was studied both under physiological conditions at pH 7.4, as well as in 20% acetic acid, pH 2, where insulin has been reported to be monomeric (*12*, *13*). Furthermore, fibril formation was studied at low pH in hydrochloric acid, where a mixture of monomers and dimers are prevalent.

It is known from the production and purification of insulin that exposure of the protein to low pH values (pH 1−3) does not cause any irreversible distortion of the native structure (*3*). In this study, low pH values were used because fibril formation under these aqueous conditions was much faster than at neutral pH (*9*). Exposure of proteins to acidic pH and high temperatures may result in significant chemical degradation. Deamidation at Asn^{A21} has been shown to be the main degradation product of insulin at pH 1.6 (*14*). Even though some deamidation is expected under some of the conditions studied, this is considered to be of minor importance, since the deamidated form of insulin has the same fibrillation properties and structural properties as the native insulin (*15*).

The kinetics of fibril formation can be described as a nucleation-dependent mechanism involving two steps, nucleation and fibril elongation (*16*, *17*). Nucleation is viewed as the assembly of several protein monomers to form an organized structure, the nucleus, as a precursor for formation of fibrils. The lag time of fibril formation is related to the time necessary for the formation of a "stable" nucleus. Subsequent addition of monomers to the nucleus elongates the nucleus into fibrils (*16*). The rate of elongation, e.g., rate of fibril growth, can be described by an apparent first-order rate constant, k_{app}. The nucleation-dependent mechanism has been found to describe the fibrillation of several proteins, including amyloid β-protein-(1−40) (*18*) and α-synuclein (*19*).

In the present investigation, the structural properties of 20 human insulin mutants (zinc-free) were studied by circular dichroism (CD) and fluorescence spectroscopy, and their tendencies to form fibrils were investigated by using the fluorescent dye, Thioflavin T (ThT). ThT has been shown to bind to insulin fibrils giving rise to a new excitation maximum at 450 nm and increased emission at 482 nm (*20*). The primary goal of the study was to investigate whether any correlation exists between the structural properties of the mutants and their fibril formation tendencies. Another purpose was to identify the specific amino acid residues involved in the interactions in fibrillar insulin in order to elucidate the molecular mechanism of insulin fibril formation.

MATERIALS AND METHODS

Materials. All insulin species studied were zinc-free unless otherwise stated. Monocomponent bovine insulin (batch 9601331) and human insulin (batch HO1713) were obtained from Novo Nordisk A/S, Denmark. Zinc content of both

species was 0.4% (w/w of insulin), corresponding to approximately 2 Zn^{2+}/insulin hexamer. Human zinc-free insulin (batch 900927) with less than 0.005% zinc (w/w of insulin) was obtained from Novo Nordisk A/S, Denmark. Zinc-free des-(B1,B2)-insulin was provided by Institut für Biochemie, Rheinisch-Westfälische Technische Hochschule, Aachen, Germany. All other human insulin mutants with one or multiple substitutions were obtained from Novo Nordisk A/S, Denmark. The mutants contained less than 0.03% zinc (w/w of insulin). Thioflavin T (ThT) and 1-anilinonaphthalene-8-sulfonic acid (ANS) were obtained from Sigma, St. Louis, MO. All other chemicals were of analytical grade from FisherChemicals.

Preparation of Insulin Samples. All insulin samples were prepared immediately prior to the kinetic experiments. ANS binding, acrylamide quenching, and CD spectroscopy were performed within 3 days of sample preparation. Insulin was dissolved at a concentration of 2 mg/mL in the appropriate buffer, and the insulin concentration was measured by UV absorption at 276 nm using an extinction coefficient of 1.08 for 1.0 mg/mL (*21*). The extinction coefficients (ϵ) for the insulin mutants were calculated from their amino acid sequences (*22*). With the exception of the mutants in which one of the four tyrosine residues was substituted, all the mutants had extinction coefficients within 10% of the wild-type. The Tyr mutants had ϵ values of 0.84 (Thr^{B26}) and 0.81 (Glu^{B16},Glu^{B27}). For intrinsic fluorescence measurements, the protein concentration was 0.2 mg/mL. Fibril formation of insulin was studied in three different media: 20% acetic acid, 0.1 M NaCl, pH 2.0 was used as the monomer condition, and 20 mM Tris, 0.1 M NaCl, pH 7.4 as the physiological condition. In addition, fibril formation in 0.1 M HCl, 0.1 M NaCl, pH 1.6 was studied. Sodium chloride was added to obtain the same ionic strength in all samples, and to accelerate the fibrillation process.

Fibril formation of insulin in hydrochloric acid and acetic acid solutions was studied in situ using ThT fluorescence. The insulin samples were incubated with 20 μM ThT in 96 microwell plates with flat bottoms (Nunc, Denmark) using a sample volume of 200 μL in each well. Five replicates corresponding to five wells were measured for each sample in order to minimize the well-to-well variation. The plate was covered by ELAS septum sheet made of Santoprene thermoplastic rubber (Spike International, Ltd., NC) and incubated at 60 °C without agitation or at 37 °C with shaking of the plate. At 37 °C, the agitation was continuous, except for readings at 15 min intervals. Insulin adsorption to the plates was investigated by incubating an insulin solution in the plate for 10 min at 37 °C with stirring, and measuring the insulin concentration by UV absorption before and after incubation. Control experiments showed that the presence of 20 μM ThT in situ had negligible effect on the kinetics of fibril formation. In addition, preincubation of ThT at 60 °C for 3 days had no effect on the signal when used in the ThT fluorescence assay, indicating that incubation of ThT in the plate-well assay at temperatures as high as 60 °C did not introduce artifacts due to dye decomposition.

Fibril formation of insulin at neutral pH required mechanical agitation of the solutions for fibrils to form within a reasonable time scale. The neutral insulin samples were incubated in glass vials at 37 °C with stirring, 0.5 mL of each neutral insulin sample was incubated in 1.8 mL borosilicate glass vials with rubber-lined closures (Fisherbrand). The solutions were stirred with micro stirring bars (8 mm × 1.5 mm, Fisherbrand). At appropriate time intervals, aliquots of 10 μL were withdrawn from the solutions, gently shaking the vial to distribute fibrils evenly in the vial before withdrawal of the aliquot. The aliquots were added to a ThT reaction mixture for fluorescent measurements.

To determine whether preexisting seeds or nuclei were present in the insulin preparations we investigated the effect of filtration through 20 nm membranes or a short pH 11 pulse prior to the start of incubation: previous studies have shown that insulin fibrils dissolve rapidly at pH 11 (*9*, *23*). These control experiments were carried out using 96-well plates at either 37 °C with shaking or at 43 °C without shaking.

Thioflavin T Fluorescence Spectroscopy. A stock solution of ThT was prepared at a concentration of 1 mM in double-distilled water and stored at 4 °C protected from light to prevent quenching until usage. For in situ ThT fluorescence measurements, 20 μM ThT was added to each of the insulin solutions to be incubated in the 96 well plate; 200 μL sample volume was added to each well. The plates were removed from the incubation at 60 °C every 30 min and fluorescence measurements were performed on a Perkin-Elmer LS 50B spectrofluorometer using the plate reader. The excitation wavelength was 450 nm, and the emission wavelength was 482 nm. Both the excitation and the emission slits were maintained at 2.5 nm. The read time for each well was 1 s (and the total read time for the whole plate was approximately 3 min).

For monitoring the fibril formation in glass vials, 10 μL aliquots were withdrawn from the glass vials and added directly to the fluorescence cuvette containing 1 mL of ThT reaction mixture (5 μM Thioflavin T, 50 mM Tris buffer, and 100 mM NaCl, pH 7.5). Fluorescence measurements were performed in semimicro quartz cuvettes (Hellma, Germany) with a 1 cm excitation light path using a FluoroMax-2 spectrofluorometer (Instruments S. A., Inc. Jobin Yvon-Spex). The light source was a 150 W xenon lamp. Emission spectra were recorded immediately after addition of the aliquots to the ThT mixture from 470 to 560 nm with excitation at 450 nm, an increment of 1 nm, an integration time of 1 s, and slits of 5 nm for both excitation and emission. For each sample, the signal was obtained as the ThT intensity at 482 nm subtracted a blank measurement recorded prior to addition of insulin to the ThT solution. Data were processed using DataMax software.

Circular Dichroism Spectroscopy. CD spectra were obtained at 23 or 60 °C on an AVIV 60DS circular dichroism spectrophotometer (Lakewood, NJ) using an insulin concentration of 2 mg/mL. In the near-UV region, CD spectra were recorded in either 0.4 or 1 cm cells from 320 to 250 nm with a step size of 0.5 nm, a bandwidth of 1.5 nm, and an averaging time of 5 s. In the far-UV region CD spectra were recorded in a 0.01 cm cell from 250 to 190 nm with a step size of 0.5 nm, a bandwidth of 1.5 nm, and an averaging time of 5 s. For all spectra, an average of 5 scans were obtained. CD spectra of the appropriate buffer were recorded and subtracted the protein spectra. The molar ellipticity, θ was calculated as the CD signal × MW (Da)/[number of residues × insulin concentrated (mg/mL) × cell path length (mm)].

ANS Binding. A fresh 10 mM ANS stock solution was prepared in double distilled water for each day of experiments. The concentration of ANS was determined by UV absorption at 350 nm using a molar extinction coefficient of 5000. An aliquot of 1 μL of the ANS solution was added to 1 mL of buffer at the appropriate pH to a final concentration of 10 μM. A blank spectrum without protein was recorded before 10 μL of insulin solution was added to the solution to a final insulin concentration of 0.02 mg/mL ($\sim$3.4 μM). Fluorescence measurements were performed immediately after the addition of insulin to the ANS solution in semimicro quartz cuvettes (Hellma, Germany). Spectra were recorded at ambient temperatures with a 1 cm excitation light path containing 1 mL of unstirred solution using a FluoroMax-2 spectrofluorometer (Instruments S. A., Inc. Jobin Yvon-Spex, USA). The light source was a 150 W xenon lamp. Emission spectra were recorded from 460 to 600 nm with excitation at 350 nm, an increment of 1 nm, an integration time of 1 s, and slits of 5 nm for both excitation and emission. Data were processed using DataMax software.

Acrylamide Quenching. Acrylamide quenching studies were performed by adding aliquots from a stock solution of the quencher into a cuvette containing protein solution at 0.2 mg/mL. The intrinsic fluorescence intensity was measured at 276 nm. Fluorescence intensities were corrected for dilution effects. Fluorescence quenching data were analyzed using the general form of the Stern−Volmer equation, taking into account not only dynamic, but also static quenching (*24*):

$$\frac{I_o}{I} = (1 + K_{SV}[Q])e^{V[Q]} \quad (1)$$

where I_o and I are the fluorescence intensities in the absence and presence of quencher, K_{SV} is the dynamic quenching constant (Stern−Volmer constant), while V is a static quenching constant, and [Q] is the total quencher concentration.

Small-Angle X-ray Scattering (SAXS). Small-angle X-ray scattering (SAXS) measurements were made using the SAXS instrument on Beam Line 4-2 at Stanford Synchrotron Radiation Laboratory. Scattering patterns were recorded by a linear position-sensitive proportional counter, which was filled with an 80% Xe/20% CO_2 gas mixture. Scattering patterns were normalized by incident X-ray intensity, which was measured with a short length ion chamber before the sample. The sample-to-detector distance was calibrated to be 230 cm, using a cholesterol myristate sample. To avoid radiation damage of the sample, the protein solution was continuously passed through a 1.3 mm path-length observation flow cell with 25 μm mica windows. Background measurements were performed before and after each protein measurement and then averaged before being used for background subtraction. All SAXS measurements were performed at 23 $\pm$ 1 °C.

The values of radii of gyration (R_g) were calculated according to the Guinier approximation (*25*):

$$\ln I(Q) = \ln I(0) - R_g^2 Q^2/3 \quad (2)$$

where Q is the scattering vector given by $Q = (4\pi \sin \theta)/\lambda$ (2θ is the scattering angle, and λ is the wavelength of X-ray). The value of I (0), the forward scattering amplitude $I(Q)$ as $Q \rightarrow 0$, is proportional to the square of the molecular weight of the molecule (*25*). I (0) for a pure dimer sample will therefore be twice that for a sample with the same number of monomers since each dimer will scatter four times as strongly, but there will be half as many as in the pure monomer sample.

Transmission Electron Microscopy (TEM). Samples of insulin fibrils were placed onto glow discharged carbon grids, rinsed with 0.1 M KCl, and negatively stained with uranyl acetate. The specimens were viewed and images recorded with a Philips 208 electron microscope operated at 80 kV.

Kinetics of Fibril Formation. The kinetics of insulin fibril formation could be described as sigmoidal curves defined by a certain lag time where little change in ThT fluorescence intensity was observed, a sigmoidal increase in ThT fluorescence denoting the growth of fibrils, and a plateau with a constant ThT fluorescence intensity indicating the end of fibril formation. ThT fluorescence measurements were plotted as a function of time and fitted to the sigmoidal curve described by the following equation using SigmaPlot,

$$F = (F_i + m_i t) + (F_f + m_f t)/(1 + \exp - (t - t_m)/\tau \quad (3)$$

where F is the fluorescence intensity, and t_m is the time to 50% of maximal fluorescence is reached. The initial baseline during the lag time is described by $F_i + m_i t$. The final baseline after the growth phase has ended is described by $F_f + m_f t$. The apparent rate constant, k_{app} for the growth of fibrils is given by $1/\tau$, and the lag time is calculated as $t_m - 2\tau$. Although eq 3 gave very good fits for the ThT kinetics profiles, the expression is strictly a simple empirical means of providing kinetics parameters for comparing rates of fibrillation from different samples, and does not directly reflect the underlying complex kinetic scheme.

RESULTS

Determination of the Association State of Insulin under Different Conditions. The association state of bovine and human insulin in different media was determined by SAXS (Table 1). In hydrochloric acid (pH 1.6), insulin is associated into dimers with an R_g of 14.9 Å. At pH 3.0, insulin has an R_g of 17.8 Å corresponding to tetramers, and at pH 7.4 insulin (with zinc) is associated into hexamers with an R_g of 19.8 Å. In 20% acetic acid, insulin is completely dissociated into monomers with an R_g of 11.8 $\pm$ 0.2 Å, regardless of species and whether zinc is present or not. Interestingly, this R_g value is very close to that calculated from the crystal structure of the hexamer for natively folded monomeric insulin (11.4 Å). Thus, the results demonstrate that insulin in 20% acetic acid is monomeric and possesses a compact nativelike structure. Finally, two human insulin mutants, Asp^{B9} + Glu^{B27} and Asp^{B28}, previously shown to be monomeric under neutral conditions (*11*), are also shown to be compact and monomeric at pH 7.4, as well as in 20% acetic acid, pH 2.0 (see Table 1).

The association state of bovine and human wild-type insulin as a function of pH is quite interesting, ranging from the hexamer at neutral pH to the monomer at pH 2 in 20% acetic acid. The reason for insulin being dimeric at pH 1.6 in HCl, and monomeric in acetic acid at pH 2.0, is not clear, but may reflect the strong hydrogen-bonding properties of carboxylic acids.

Table 1: Effects of pH on the Association State of Insulin Determined by Small-Angle X-ray Scattering[a]

insulin species	pH	condition	R_g (Å)	association state[b]
bovine	1.6	25 mM HCl, 100 mM NaCl	14.9 ± 0.1	2.14
bovine	3.0	20 mM formate, 100 mM NaCl	17.8 ± 0.1	4.28
bovine	7.4	20 mM phosphate, 100 mM NaCl	19.8 ± 0.1	5.93
bovine	2.0	20% acetic acid, 100 mM NaCl	11.6 ± 0.2	1.02
human	2.0	20% acetic acid, 100 mM NaCl	12.0 ± 0.2	1.17
human, zinc-free	2.0	20% acetic acid, 100 mM NaCl	11.8 ± 0.2	1.23
Asp^{B28} insulin mutant	2.0	20% acetic acid, 100 mM NaCl	11.3 ± 0.2	1.17
Asp^{B28} insulin mutant	7.4	20 mM phosphate, 100 mM NaCl	11.2 ± 0.2	1.25
Asp^{B9}, Glu^{B27} insulin mutant	2.0	20% acetic acid, 100 mM NaCl	11.7 ± 0.2	1.00
Asp^{B9}, Glu^{B27} insulin mutant	7.4	20 mM phosphate, 100 mM NaCl	11.1 ± 0.2	1.30

[a] The insulin concentration was 2 mg/mL. [b] The association state was calculated from the $I(0)/I(0)_{\text{monomeric insulin}}$ corrected for differences in concentration.

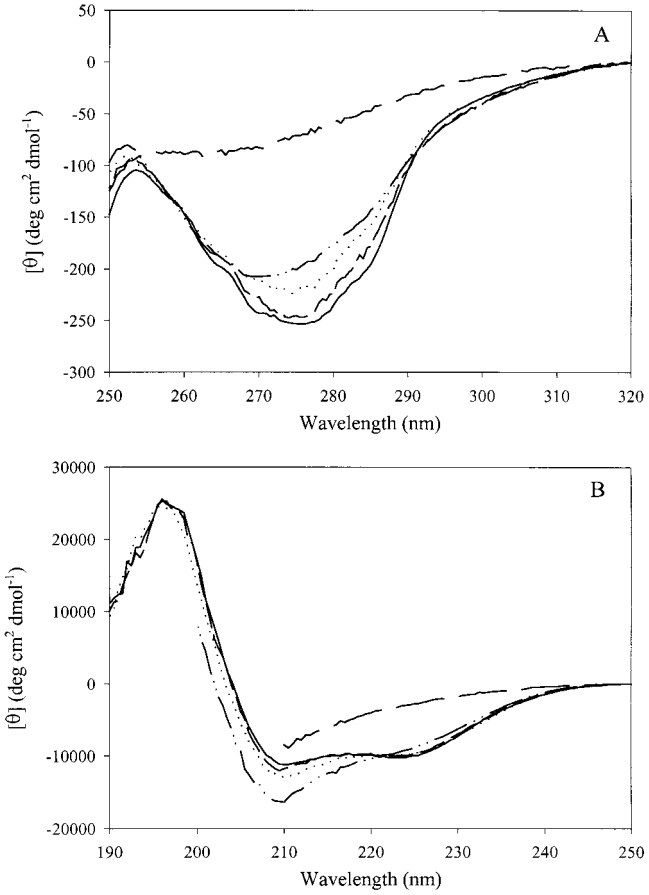

FIGURE 2: Near-UV CD (A) and far-UV CD (B) spectra of human insulin with zinc in different association states. Insulin concentration was 2 mg/mL in 20% acetic acid, 0.1 M NaCl, pH 2 (dot−dashed line), 0.025 M HCl, 0.1 M NaCl, pH 1.6 (dotted line), 20 mM formate, 0.1 M NaCl, pH 3 (dashed line), Tris, pH 7.4 (solid line), and 8 M urea (long-dashed).

The near- and far-UV CD spectra of human insulin in different association states are shown in Figure 2. Spectra of unfolded insulin (8 M urea) are also shown for comparison. It is evident that the shape and intensity of the near-UV−CD spectra are sensitive to the pH and solvent (Figure 2A). However, even under conditions of extremely low pH, insulin shows a significant near-UV−CD spectrum. This indicates that under all the conditions studied (with the exception of 8 M urea, where insulin is unfolded) insulin retains a compact and a relatively nativelike tertiary structure, even at low pH. A decrease in pH leads to minor changes in the shape of the far-UV−CD spectrum of insulin, indicating only small changes in the secondary structure (Figure 2B). Notably, the largest effect was observed in acetic acid under monomeric conditions.

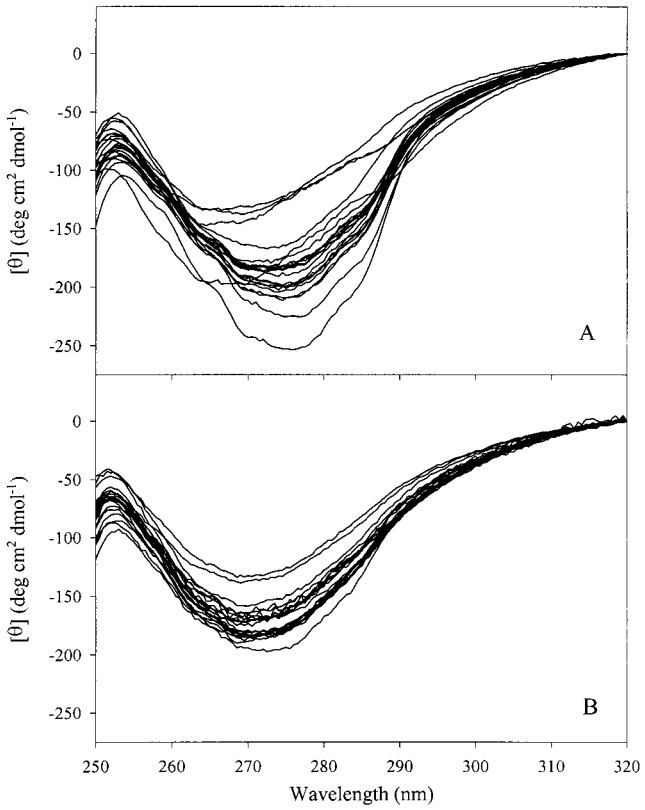

FIGURE 3: Near UV−CD spectra of 2 mg/mL human insulin mutants in 20 mM Tris, 0.1 M NaCl, pH 7.4, 1 cm path length cell (A), and in 20% acetic acid, 0.1 M NaCl, pH 2.0, 0.4 cm path length cell (B). The order of the mutants with increasing negative ellipticity at 275 nm (A) was Thr^{B26} < Asp^{B25} < Asp^{B9}+Glu^{B27} < Glu^{B16}+Glu^{B27} < Ser^{A13}+Glu^{B27} < Asp^{B10} = Glu^{A13}+Glu^{B10}= $des^{B1,B2}$ < Ala^{B17} < Glu^{B1}+Glu^{B27} < Ser^{B2}+Asp^{B10} < bovine < Asp^{B28} = Val^{A10} < Gln^{B17} < Glu^{A15}+Asp^{A18}+Asp^{B3} < Ser^{A13}+Gln^{A17}+Glu^{B10}+Gln^{B17}+des^{B3} < human, zinc-free < Glu^{B27} = Gln^{B18} < His^{A8} < human with zinc. The order of the mutants with increasing negative ellipticity at 270 nm (B) was Glu^{B27} < Asp^{B9}+Glu^{B27} < Glu^{A15}+Asp^{A18}+Asp^{B3} < Gln^{B17} < human, zinc-free = human with zinc < Thr^{B26} = $des^{B1,B2}$ < Ser^{A13}+Gln^{A17}+Glu^{B10}, Gln^{B17}, des^{B3} < Ala^{B17} < Asp^{B28} < His^{A8} < Glu^{B1}+Glu^{B27} < Gln^{B18} < bovine = Ser^{B2}+Asp^{B10} = Val^{A10} < Glu^{A13}+Glu^{B10} < Asp^{B25} = Asp^{B10} < Ser^{A13}+Glu^{B27} < Glu^{B16}+Glu^{B27}.

Tertiary Structure of the Insulin Mutants. All the insulin samples are characterized by significant near-UV CD spectra under all the conditions studied, indicating that the overall tertiary structure of insulin is not dramatically affected by the amino acid substitutions (or the pH) (Figure 3). However, at neutral pH, the spectra reveal significant differences in the tertiary structure of many of the insulin mutants (Figure 3A). Except for the Thr^{B26}, Asp^{B9}+Glu^{B27}, and Asp^{B28}

mutants, which show minima at 265 nm, all the mutants exhibit minima at 275 nm. The ellipticity at 275 nm for all the mutants varies in the range from −122 to −253 deg cm^2 dmol^{-1}. Human insulin with zinc exhibits the largest negative CD signal at 275 nm, indicating the most structured conformation, probably due to the stabilizing effect of zinc on the hexamer conformation. The His^{A8} mutant also exhibits a strong negative signal at 275 nm. The proteins showing the weakest signal at 275 nm are the Thr^{B26}, Asp^{B25}, and Asp^{B9}+Glu^{B27} insulin mutants. The rest of the mutants as well as bovine and zinc-free human insulin exhibit CD signals at 275 nm ranging from −165 to −210 deg cm^2 dmol^{-1}.

The near-UV−CD spectra measured for the insulin mutants in 20% acetic acid, pH 2.0, show that all the mutants have significant nativelike tertiary structure (Figure 3B). The spectra are more similar to each other than those measured at pH 7.4. All the spectra in 20% acetic acid show minima at 270 nm, and the intensities vary in the range from −134 to −208 deg cm^2 dmol^{-1}. The Glu^{B16}+Glu^{B27} mutant exhibits the strongest negative CD signal, whereas the Glu^{B27} and Asp^{B9}+Glu^{B27} mutants have the weakest intensities at 270 nm. The remaining mutants as well as human insulin with and without zinc have CD signals at 270 nm ranging from −159 to −188 deg cm^2 dmol^{-1}.

Fluorescence Spectroscopy of the Insulin Mutants. Fluorescence spectroscopy also shows that the insulin mutants retain relatively nativelike structure. First of all, no change in ANS fluorescence intensity or emission maximum upon addition of any of the insulin mutants to ANS solution was seen at either pH 1.6, 2.0, or 7.4 (data not shown). This indicates that none of the proteins have significant solvent-accessible hydrophobic surfaces under any of the conditions studied. Thus, at low protein concentrations (∼0.02 mg/mL) there is no evidence for the presence of significant concentrations of any partially folded intermediate, at least one that binds ANS. Furthermore, since the insulin mutants show little interaction with ANS under these conditions, no significant structural changes are induced by either the point mutations or acidification of the solution.

Insulin contains four tyrosines, Tyr^{A14}, Tyr^{A19}, Tyr^{B16}, and Tyr^{B26}, but no tryptophan residues. Unlike tryptophan fluorescence, the position of maximal emission of tyrosine is insensitive to the polarity of the environment. However, the intensity of tyrosine fluorescence emission is extremely sensitive to the chromophore microenvironment (*26*). The fluorescence analysis of the insulin mutants at neutral pH and in 20% acetic acid, pH 2.0, is shown in Figure 4. The intensity of intrinsic tyrosine fluorescence of the insulin mutants at neutral pH varies significantly, with almost a 2-fold difference between the lowest and highest signal (Figure 4A). This indicates that the environment of the tyrosines in the mutants varies either due to changes induced by the point mutations or due to different degrees of self-association at pH 7.4. Under monomeric conditions in 20% acetic acid, pH 2.0, the variations in intrinsic fluorescence are smaller, probably because variations due to different association states are eliminated. Thus, the differences seen in acetic acid are caused by changes in the environment of the tyrosine residues induced by the mutations.

To provide more information about the environment of the tyrosines, we investigated the efficiency of their fluorescence quenching by the neutral quencher acrylamide. The

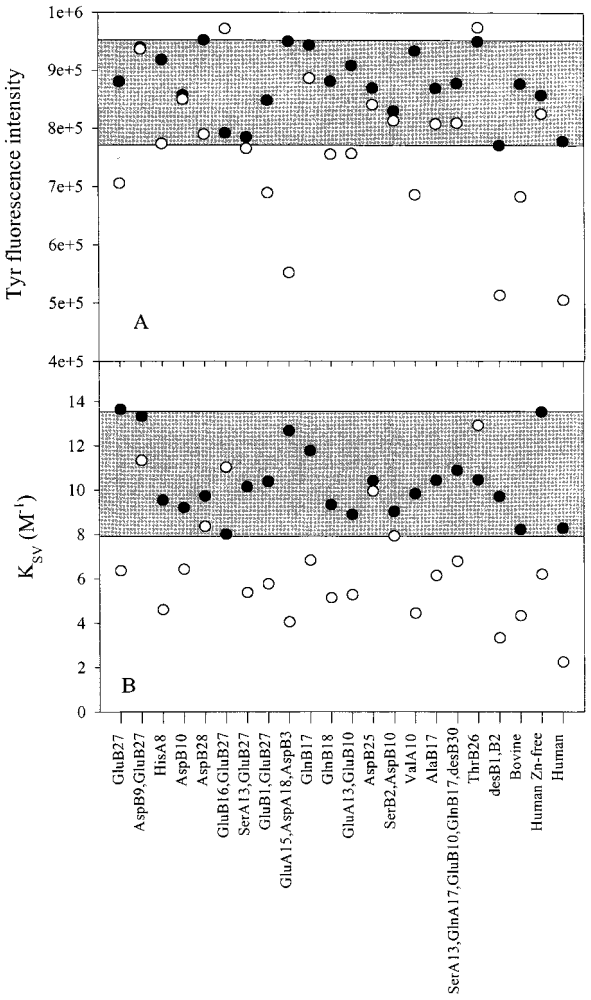

FIGURE 4: Intrinsic tyrosine fluorescence intensity (at 305 nm) (A) and Stern−Volmer constants (B) of human insulin mutants in 20 mM Tris, 0.1 M NaCl, pH 7.4 (open symbols) and in 20% acetic acid, 0.1 M NaCl, pH 2.0 (black symbols, located in shaded region). Insulin concentration was 2 mg/mL.

Stern−Volmer constants, calculated from eq 1, are generally larger for the insulin mutants in acetic acid than those determined at neutral pH. Thus, in the monomeric state the tyrosines are more accessible to acrylamide, indicating that the monomeric conformation is more flexible compared to the more associated states at neutral pH. Furthermore, the values of the Stern−Volmer constant show less variation under these conditions. This may be explained by the fact that all the mutants are monomeric in 20% acetic acid, pH 2.0, whereas at neutral pH they range from monomers to tetramers, resulting in greater variability of the fluorescence quenching, due to decreased mobility in the associated species.

The accessibility of tyrosine residues in the insulin mutants is compared with the intensity of the corresponding near-UV CD signals in Figure 5. Under both conditions, smaller negative ellipticities at 275 nm correspond to larger Stern−Volmer constants indicating that mutants with the most accessible tyrosines have the least intense near-UV−CD spectra. This correlation between K_{SV} and $[\theta]_{275}$ is much more pronounced for the mutants under monomeric conditions in acetic acid, probably due to the absence of contributions from protein self-association.

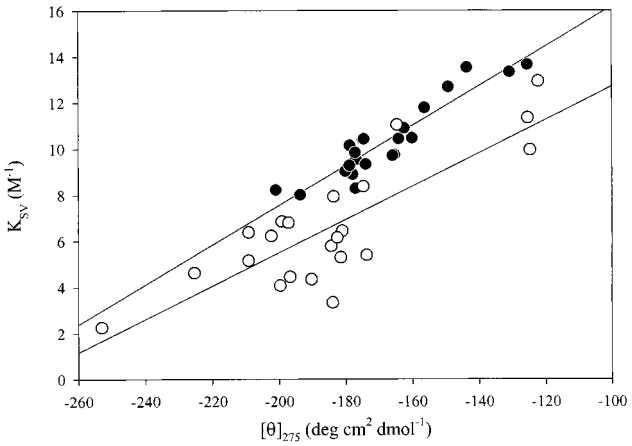

FIGURE 5: Correlation between Stern−Volmer constants and molar ellipticity at 275 nm of human insulin mutants in 20 mM Tris, 0.1 M NaCl, pH 7.4 (open symbols) and in 20% acetic acid, 0.1 M NaCl, pH 2.0 (black symbols). Insulin concentration was 2 mg/mL.

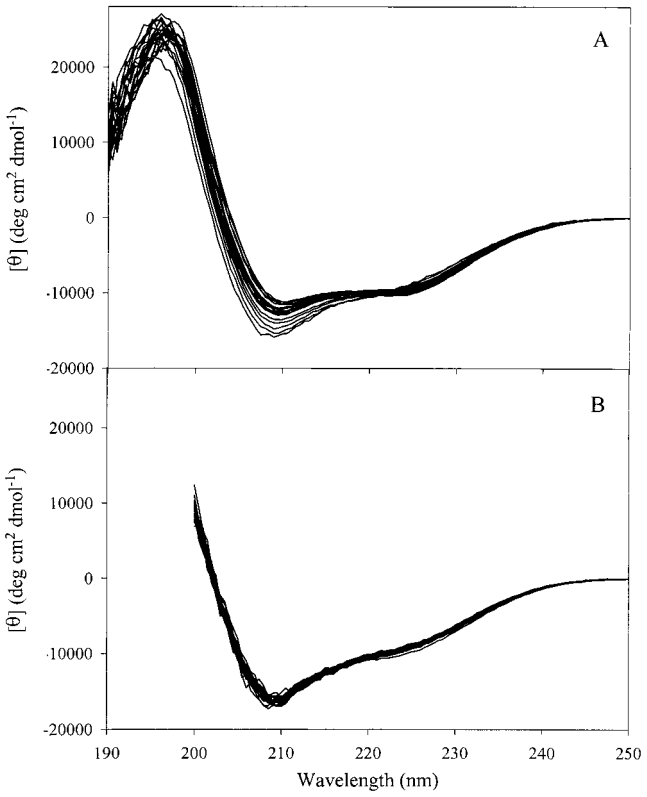

FIGURE 6: Far UV−CD spectra of 2 mg/mL human insulin mutants in 20 mM Tris, 0.1 M NaCl, pH 7.4, 1 cm path length cell (A), and in 20% acetic acid, 0.1 M NaCl, pH 2.0, 0.4 cm path length cell (B). The order of the mutants with increasing negative ellipticity at 208 nm (A) was Human with zinc < Ser^{A13}+Gln^{A17}+Glu^{B10}+Gln^{B17}+des^{B30} < Glu^{A13}+Glu^{B10} < His^{A8} < Gln^{B17} < Ala^{B17} < Gln^{B18} < Glu^{B27} < Asp^{B10} < human, zinc-free < Ser^{A13}+Glu^{B27} < Ser^{B2}+Asp^{B10} < $des^{B1,B2}$ < Glu^{B1}+Glu^{B27} < bovine < Val^{A10} < Glu^{A15}+Asp^{A18}+Asp^{B3} < Asp^{B28} < Glu^{B16}+Glu^{B27} < Asp^{B25} < Asp^{B9}+Glu^{B27} < Thr^{B26}. In acetic acid (B), the ellipticity at 208 nm is essentially the same for all mutants.

Secondary Structure of the Insulin Mutants. The far UV−CD spectra at neutral pH show minor differences in the secondary structure of the mutants (Figure 6A). The spectra of human insulin with and without zinc exhibit two minima at 208 and 222 nm characteristic of the α-helical conformation. Some of the far UV−CD spectra exhibit increased negative intensity at 208 nm and loss of the minimum at 222 nm, indicating loss of some α-helical structure (*27*). This is seen for the following mutants: Asp^{B25}, Thr^{B26}, Asp^{B28}, the double mutant Glu^{B16}+Glu^{B27}, and the triple mutant Glu^{A15}+Asp^{A18}+Asp^{B3}. In 20% acetic acid, all the mutants have identical far UV−CD spectra with a strong negative minimum at 208 nm and a weaker minimum at 222 nm indicating identical secondary structure (Figure 6B). The relative increase in the negative ellipticity at 208 nm observed for all insulins in acetic acid indicates some loss in α-helical structure. Table 2 summarizes the structural properties of the insulin mutants resulting from the CD and fluorescence spectroscopic analyses. Note that most of the mutants at the concentrations used are mixtures of dimers and tetramers at neutral pH, and some are monomers.

Propensity for Fibrillation of the Insulin Mutants. All the human insulin mutants were tested for their tendencies to form fibrils in acetic acid (monomeric conditions) and in hydrochloric acid (mixture of monomers and dimers) and some also at physiological pH (insulin self-associating conditions). During the lag phase of fibril formation, no significant changes in ThT fluorescence are observed. As fibrils are formed, the ThT fluorescence intensity at 482 nm increases as a function of time as shown for representative insulin mutants in Figure 7. The curves for each mutant were fitted using eq 3, and the lag times and apparent rate constants were calculated for fibrillation both in acetic acid, pH 2.0, hydrochloric acid, pH 1.6 and at neutral pH (Table 3). TEM analysis shows that, at the final stage (at the time-points corresponding to the upper plateau of the sigmoidal increase in ThT fluorescence intensity), all insulin mutants had formed fibrils. Representative examples of TEM of fibrils are shown in Figure 8.

To ensure that the differences in rate of fibril formation by the different mutants did not arise from the presence of preexisting seeds or nuclei (which would result in faster rates of fibril formation), we compared the effects of no treatment, ultrafiltration, and a pulse of high pH on the kinetics of fibril formation. The latter two conditions should remove any fibril seeds present. Since treatment of the insulin samples with either method did not result in longer lag times, we conclude that there were negligible amounts of seeds or nuclei present in the preparations.

Both in acidic and neutral media, the rate of fibril formation at 37 °C was significantly enhanced by stirring the solutions (data not shown). Alternatively, in the absence of agitation, fibril formation was accelerated by raising the temperature to 60 °C for the acidic samples. However, fibril formation at neutral pH required stirring or agitation to have fibrils formed within 24 h at 60 °C (data not shown). It has previously been shown that insulin aggregation at neutral pH only occurred when agitation and hydrophobic surfaces were present (*28*). Therefore, fibril formation at neutral pH was performed at 37 °C in glass vials, which made it possible to stir each individual sample uniformly.

At neutral pH, all the insulin mutants form fibrils with shorter lag times (5−43 h) than human insulin (49 h) as seen in Table 3. Bovine insulin (with 2 Zn^{2+}/hexamer) forms fibrils with a 7-fold shorter lag time than human insulin with zinc. Only the mutant Ser^{A13}+Glu^{B27} has a shorter lag time than bovine insulin. All mutants at neutral pH are less

Table 2: Structural Properties of Human Insulin and Insulin Mutants at pH 7.4 and pH 2.0

		20 mM Tris, 0.1 M NaCl, pH 7.4				20% acetic acid, 0.1 M NaCl, pH 2.0		
human insulin mutants	substitutions	association state[b]	K_{SV} (M^{-1})	$[\theta]_{208}/[\theta]_{222}$ (deg cm^2 dmol^{-1})	$[\theta]_{275}$ (deg cm^2 dmol^{-1})	K_{SV} (M^{-1})	$[\theta]_{208}/[\theta]_{222}$ (deg cm^2 dmol^{-1})	$[\theta]_{270}$ (deg cm^2 dmol^{-1})
human, Zn^{2+} free		4.4	6.21	0.97	−202	8.29	1.56	−166
human, 2 Zn^{2+}/hexamer		6[c]	2.25	1.17	−253	13.53	1.58	−166
bovine[a]		6[c]	4.33	1.21	−190	8.22	1.57	−183
dimer interface								
Asp^{B25}	Phe→Asp	2.2	9.95	1.38	−125 (−137[d])	10.42	1.42	−185
Thr^{B26}	Tyr→Thr		12.93	1.59	−122 (−131[d])	10.46	1.74	−169
Glu^{B27}	Thr→Glu	4.0	6.37	1.12	−209	13.65	1.47	−133
Asp^{B28}	Pro→Asp	1.3[c]	8.37	1.31	−175 (−197[d])	9.73	1.56	−173
Asp^{B9}, Glu^{B27}	Ser→Asp, Thr→Glu	1.0[c]	11.34	1.48	−125 (−142[d])	13.33	1.60	−137
Glu^{B16}, Glu^{B27}	Tyr→Glu, Thr→Glu	1.1	11.03	1.35	−165	8.00	1.66	−194
hexamer interfaces								
Asp^{B10}	His→Asp	2.2	6.43	1.15	−181	9.21	1.56	−185
Ala^{B17}	Leu→Ala		6.14	1.08	−183	10.43	1.56	−172
Gln^{B17}	Leu→Gln	2.3	6.84	1.06	−199	11.77	1.58	−164
Gln^{B18}	Val→Gln		5.14	1.13	−209	9.33	1.61	−181
Ser^{A13}, Glu^{B27}	Leu→Ser, Thr→Glu	2.9	5.38	1.11	−174 (−178[d])	10.14	1.75	−188
Glu^{A13}, Glu^{B10}	Leu→Glu, His→Glu	1.9	5.28	1.03	−181	8.90	1.48	−184
Ser^{A13}, Gln^{A17}, Glu^{B10}, Gln^{B17}, des^{B30}	Leu→Ser, Glu→Gln, His→Glu, Leu→Gln, B30-des		6.79	0.97	−201	10.89	1.39	−171
intermolecular β-sheet[e]								
Glu^{B1}, Glu^{B27}	Phe→Glu, Thr→Glu	2.6	5.77	1.20	−184	10.39	1.44	−180
Ser^{B2}, Asp^{B10}	Val→Ser, His→Asp	2	7.93	1.18	−184	9.03	1.52	−183
$des^{B1,B2}$	des-(B1,B2)		3.33	1.22	−181	9.27	1.55	−169
other mutations								
Glu^{A15}, Asp^{A18}, Asp^{B3}	Gln→Glu, Asn→Asp, Asn→Asp		4.06	1.29	−200	12.68	1.58	−159
His^{A8}	Thr→His		4.61	1.05	−225	9.54	1.57	−179
Val^{A10}	Ile→Val		4.44	1.25	−197	9.84	1.49	−183

[a] Bovine insulin differs from human insulin at the following residues: Thr^{A8}→Ala, Ile^{A10}→Val, Thr^{B30}→Ala. [b] Data determined at 1 mM by osmometry (*11*). [c] Data from SAXS analysis. [d] $[\theta]_{270}$. [e] According to the insulin fibril model (*7*).

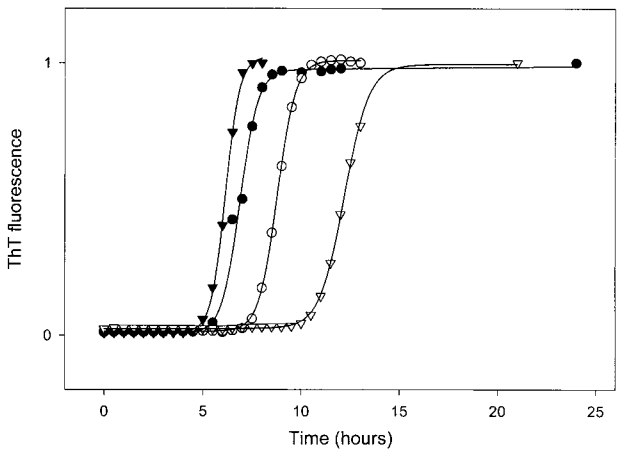

FIGURE 7: Fibril formation of human insulin and insulin mutants at concentrations of 2 mg/mL in 20% acetic acid, 0.1 M NaCl, pH 2 monitored by in situ Thioflavin T binding. The insulin species were Human zinc-free insulin (●), Gln^{B18} (○) Ser^{A13}+Glu^{B27} (▼), and Val^{A10} (▽). The fluorescence intensities were normalized on a scale from zero to one.

associated (mostly monomers and dimers) than the zinc-free human insulin. This correlates well with the observed shorter lag times for the mutants compared to the more associated human insulin. However, there is no correlation between the initial degree of association of the mutants and their lag times at pH 7.4 (Tables 2 and 3).

At 37 °C with stirring, the lag time for wild-type human insulin fibril formation was 15-fold shorter at pH 1.6 than at pH 7.4 (data not shown). Therefore, it is not surprising that the mutants exhibit shorter lag times at acidic pH compared to neutral pH (Table 3). In both acidic media, only a few of the mutants have shorter lag times than the wild-type protein. In acetic acid, the mutants Ser^{A13}+Glu^{B27}, Glu^{B1}+Glu^{B27}, Glu^{B27}, and Asp^{B28}, as well as bovine insulin, have similar lag times as human insulin. All the other mutants had up to 3-fold longer lag times for fibril formation compared to human zinc-free insulin in acetic acid. In HCl, only two mutants (Ser^{A13}+Glu^{B27} and Glu^{B1}+Glu^{B27}), as well as bovine insulin, form fibrils significantly faster than the wild-type human protein. Four mutants are moderately faster than human insulin, the monosubstituted analogues Glu^{B27} and Ala^{B17}, the double mutant Glu^{B16}+Glu^{B27}, and the mutant with four substitutions Ser^{A13}+Gln^{A17}+Glu^{B10}+Gln^{B17}+des^{B30}. The remaining mutants all have up to 3-fold longer lag times for fibril formation than human zinc-free insulin. In both acidic media, mutants with the single mutations Asp^{B10} and Gln^{B17} are the slowest fibril forming species. It is noteworthy that the differences in lag times for the mutants and the wild-type human insulin are less pronounced in both acidic media compared to neutral pH.

DISCUSSION

Correlation between Degree of Association and Propensity of Fibril Formation. Comparison of the lag times for human insulin in the hexameric two-zinc form and the zinc-free tetrameric form at physiological pH indicates that the former has a longer lag time, suggesting that dissociation from the more tightly associated hexamer contributes to the nucleation

Table 3: Kinetics of Fibril Formation of Native Insulins and Insulin Mutants at pH 7.4, 2.0, and 1.6

human insulin mutants	substitutions	fibrillation at pH 7.4, 37 °C[a] lag time (h)	k_{app} (h^{-1})	fibrillation at pH 2.0, 60 °C lag time (h)	k_{app} (h^{-1})	fibrillation at pH 1.6, 60 °C lag time (h)	k_{app} (h^{-1})
human, Zn^{2+} free		49.4	0.2	6.1 ± 0.4 ($n = 5$)	2.6	8.9 ± 0.4 ($n = 5$)	1.1
human, 2 Zn^{2+}/hexamer		60.0	0.1	5.1 ± 0.4 ($n = 5$)	2.3	7.3 ± 0.4 ($n = 5$)	1.4
bovine[b]		8.1[c]	1.7	6.3 ± 0.4 ($n = 5$)	3.0	4.2 ± 0.4 ($n = 5$)	2.6
dimer interface							
Asp^{B25}	Phe→Asp			13.2	1.3	22.7	11.9
Thr^{B26}	Tyr→Thr			10.7	1.1	10.5	0.98
Glu^{B27}	Thr→Glu			6.5	2.0	7.0	1.7
Asp^{B28}	Pro→Asp	16.5	0.3	4.8	1.3	14.5	0.47
Asp^{B9}, Glu^{B27}	Ser→Asp, Thr→Glu	20.8	4.1	10.2	2.6	10.6	2.0
Glu^{B16}, Glu^{B27}	Tyr→Glu, Thr→Glu	43.1	0.05	13.1	1.1	6.8	2.9
hexamer interfaces							
Asp^{B10}	His→Asp	24.9	0.4	20.3	0.73	>24	nd[d]
Ala^{B17}	Leu→Ala			8.9	0.9	7.8	2.1
Gln^{B17}	Leu→Gln	18.9	0.5	19.5	1.0	23.1	16.9
Gln^{B18}	Val→Gln			7.9	2.2	22.8	11.6
Ser^{A13}, Glu^{B27}	Leu→Ser, Thr→Glu	5.0	2.1	5.5	2.5	3.2	3.1
Glu^{A13}, Glu^{B10}	Leu→Glu, His→Glu	32.1	0.2	7.8	2.1	23.1	16
Ser^{A13}, Gln^{A17}, Glu^{B10}, Gln^{B17}, des^{B30}	Leu→Ser, Glu→Gln, His→Glu, Leu→Gln,B30-			8.6	1.4	7.2	2.6
intermolecular β-sheet							
Glu^{B1}, Glu^{B27}	Phe→Glu, Thr→Glu			6.2	2.7	4.0	1.7
Ser^{B2}, Asp^{B10}	Val→Ser, His→Asp	15.1	0.5	7.1	2.6	16.8	0.62
$des^{B1,B2}$	des-(B1,B2)	36.6	0.5	9.3	2	11.5	1
other mutations							
Glu^{A15}, Asp^{A18}, Asp^{B3}	Gln→Glu, Asn→Asp, Asn→Asp			15.0	0.48	23.1	10.5
His^{A8}	Thr→His			14.6	1.2	11.1	0.65
Val^{A10}	Ile→Val			10.9	1.6	23.0	15.4

[a] Stirred solution. [b] Bovine insulin differs from human insulin at the following residues: Thr^{A8}→Ala, Ile^{A10}→Val, Thr^{B30}→Ala. [c] No fibrils were formed at 60 °C without stirred solution within 24 h. [d] nd, not determined.

kinetics. This observation is consistent with the fibril pathway starting with monomers. Several previous studies also indicate that insulin fibril formation proceeds via monomerization of the oligomeric insulin molecules (*7*, *9*). It has also been shown in the case of transthyretin (a native tetramer) that the monomeric form of the protein was the repeating structural subunit in the amyloid fibrils (*29*).

As the human insulin mutants all have different association states at pH 7.4 (Table 2) (*11*), the kinetics of fibril formation at pH 7.4 may be complicated by dissociation of the oligomeric forms into monomers. Since insulin was shown to be monomeric in 20% acetic acid, pH 2.0, and retains a nativelike tertiary structure and compactness, these conditions were used to dissociate all the mutants into monomers for the studies of fibril formation. It is clear from the results in Table 3 that the initial oligomeric state of insulin has a significant impact on the kinetics of nucleation, as reflected in the different lag times. However, additional factors must also be involved. These presumably include the nature of the interactions between monomeric units in forming the initial oligomers leading to fibrils. This is also supported by the fact that, although the mutants studied fibrillate faster than the wild-type protein at neutral pH since they all are less associated than human zinc-free insulin (*11*), bovine insulin is the fastest fibrillating native species at neutral pH despite being in its stable hexameric conformation.

The observation that the differences in the lag times in both acidic media are less pronounced than those at neutral pH, is probably a reflection that, contrary to the conditions of neutral pH, no dissociation in acetic acid (and less dissociation in hydrochloric acid) has to occur before fibrillation. Since, under these monomeric conditions, the degree of insulin association in the initial solution (prior to initiation of fibril formation) cannot be ascribed as a factor in determining the propensity of a given insulin mutant to form fibrils, it is reasonable to suggest that differences in structural properties (tertiary and secondary structure) may represent such a factor. For reasons to be elaborated on subsequently, we propose that the monomeric form of insulin is in equilibrium with a partially folded intermediate. This intermediate is the conformation that associates to form oligomers that ultimately form the critical nucleus and fibrils. The existence of partially folded intermediates of insulin has been previously reported (*30*, *10*).

Structural Properties of the Insulin Mutants and Their Propensities to Fibril Formation. The changes in the near- and far-UV CD, and the Stern−Volmer constants for monomeric insulin, compared to the hexamer suggest that small but significant differences exist in the conformation of the insulin molecule in the monomeric state. The change in the far-UV CD signal on going from hexamer to monomer is consistent with loss of some α-helix. The SAXS data indicate that the majority of the molecules under monomeric conditions must be quite compact; however, the technique would not be able to detect a small percentage of more expanded molecules. The correlation between the Stern−Volmer constant and the ellipticity at 275 nm (Figure 5) for the mutants in the monomeric state indicates that less intense (negative) ellipticity corresponds to greater flexibility and probably more partially folded intermediate or a lower energy barrier to the intermediate from the monomer. Interestingly, there is no correlation between the flexibility of the mutants (as determined by the Stern−Volmer constant) and the lag times for fibrillation in the monomeric state.

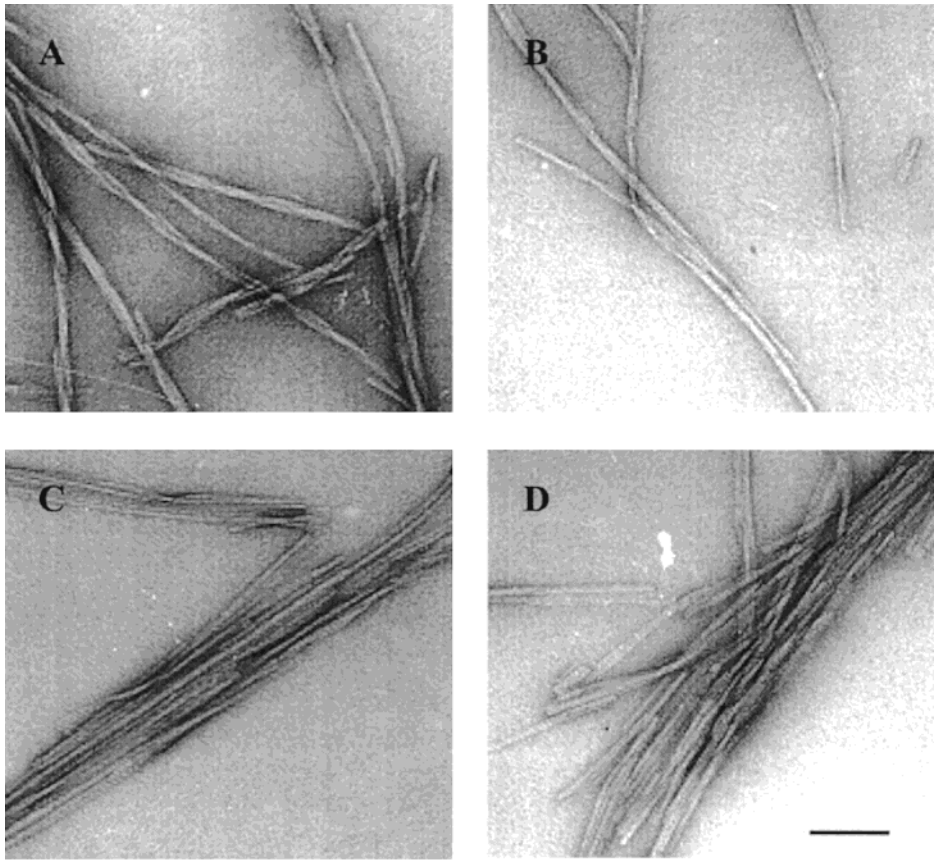

FIGURE 8: Negative staining transmission electron micrographs of insulin fibrils prepared by heating at 50 °C in 0.1 M hydrochloric acid for 20 h. (A) Glu^{B1}+Glu^{B27}, (B) $des^{B1,B2}$, (C) Asp^{B10}, and (D) human zinc-free insulin. The scale bar represents 100 nm.

All the spectroscopic data indicate that the insulin mutants preserve substantial nativelike structure under all conditions studied. However, some mutants may possess more distorted structure than others. For example, the acrylamide quenching experiments demonstrate that there are significant differences in the structures of the mutants. The differences seen in the near-UV−CD spectra and the acrylamide quenching properties of the insulin mutants can be caused by several factors. First of all, the degree of association (at neutral pH) will affect the environment of the tyrosines. An increase in the negative ellipticity around 275 nm has been shown to correspond to increased association of insulin (*31*, *12*, *13*). Second, the point mutations can also affect the local environment of the tyrosines. And third, the structural differences observed might be a direct conformational effect, which would indicate the existence of a partially folded intermediate. However, if the concentration of such an intermediate is low (less than 5−10%), then it would be difficult to detect its presence with any of the techniques employed in this study.

Although the insulin mutants show significant structural differences, the lengths of the corresponding lag times are unrelated to all the structural parameters studied. This is in contrast to a report for different forms of amyloid β-peptide, in which a direct correlation was found between the ability to form amyloid fibrils and their initial secondary structure (*32*). This means that for insulin, the structural peculiarities of the starting conformation are rather specific in terms of the propensity of a given mutant to form fibrils. There are two most likely factors involved. The first is that the nature of the intermolecular interaction in the initially formed oligomers during fibrillation will potentially be affected by the mutations in a manner specific to each mutation. The second is that if the fibrillar oligomers originate with a partially folded intermediate then the mutations might affect the amount of intermediate formed or they might perturb the structure of the intermediate thus affecting its propensity to form fibrils.

Molecular Mechanism of Fibril Formation: Incompatibility with the Model of Brange et al. (7). The majority of the human insulin mutants studied here have substitutions of surface hydrophobic residues with more hydrophilic ones. This is expected to weaken the intermolecular hydrophobic interactions and make the proteins less prone to form fibrils, if hydrophobic interactions are essential for the fibrillation and if the mutated residues are involved in the fibrillar interactions (*7*). Since surface mutations would be expected to affect self-association of nativelike conformations, the observation that the mutants are less associated at neutral pH is the expected consequence. As shown in Table 3, the mutants (with a few exceptions) have longer lag times in the acidic media compared to the wild-type zinc-free insulin. This supports the idea that insulin fibril formation, at least the initial nucleation, is mainly driven by hydrophobic interactions.

To gain further insight into the molecular mechanism of insulin fibril formation, the fibrillation tendencies of the insulin mutants may be considered in relation to the proposed model (*7*), which posits a nativelike core conformation in the individual molecules in the fibrils. In the following discussion only the data at pH 2.0 where the starting molecules are monomeric will be considered.

In the model of Brange et al. (*7*), the first set of interactions in the insulin fibril was suggested to involve hydrophobic interactions between residues A2, A3, B11, and B15 in one molecule and residues A13, B6, B14, B17, and B18 in an adjacent molecule. Substituting the long aliphatic side chain of Leu with a methyl group in B17 in the mutant Ala^{B17} had relatively little effect on the lag time, indicating that the length of the hydrophobic side chain in position B17 is not crucial for nucleation. Introduction of an amide group in B17 in the mutant Gln^{B17} involved mutation to a more polar residue without changing its charge or size. The increased lag time of the mutant Gln^{B17} suggests that the hydrophobic interactions necessary for nucleation have been disrupted. The importance of the residue B17 is in agreement with what was predicted earlier from the model of insulin fibrils (*7*, *8*). However, introducing an amide group in B18 (Gln^{B18}) had no significant effect on the lag time under monomeric conditions.

Introduction of a hydroxyl group in A13 in the mutant Ser^{A13}+Glu^{B27} had little effect on fibrillation. However, mutation of A13 to an acid (Glu^{A13}+Glu^{B10}) decreased the lag time, in comparison to the monosubstituted mutant, Asp^{B10}, which also had a carboxyl group introduced in B10. Thus, there is no evidence to prove that mutation to more hydrophilic residues in position A13 is inhibiting insulin fibril formation.

The second set of interactions in the insulin fibril was hypothesized to be an intermolecular β-sheet between B1−B5. Three mutants with substitutions in this region were investigated. Glu^{B1}+Glu^{B27} formed fibrils with similar lag times to the wild-type human protein. Since the mutant Glu^{B27} had comparable lag times (and k_{app}) with human insulin, substituting Thr to Glu in B27 is not considered to have any effect on the fibrillation tendencies of the mutants, and neither is the substitution of Phe to Glu in B1. The second mutant with substitutions in the potential intermolecular β-sheet was Ser^{B2}+Asp^{B10}. To interpret the effect of the B2 mutation, it is necessary to consider the mutation of His to Asp in B10. Asp^{B10} is seen to form fibrils with the longest lag time compared to all other mutants, indicating that the introduction of Asp in position B10 is inhibiting nucleation. Since the mutant Ser^{B2}+Asp^{B10} has shorter lag times than Asp^{B10}, the substitution of Val to the more hydrophilic Ser in B2 is considered to promote fibril formation (nucleation), indicating a promoting effect of introducing a hydroxyl group in B2.

The removal of B1 and B2 resulted in a longer lag time compared to the wild-type protein, indicating that B1 and B2 are somewhat important for the stabilization of the nucleus. According to the insulin fibril model (*7*), B1−B5 would be important for growth of the fibrils in lateral direction (perpendicular to the length axis), and therefore the removal of B1−B5 should not affect the nucleation, but rather the growth of the fibril. However, k_{app} for des-(B1,B2) insulin is not changed significantly from the wild-type protein.

Substitution of His to Asp in position B10 results in a mutant with very long lag times at low pH. Studies on the chemical reactivity of functional groups have revealed that about half of the imidazolyl groups have reduced activity in fibrillar insulin compared to native insulin (*33*). Thus, these studies indicate that His^{B10} seems to be critically involved in the interactions in the nucleation, also indicating the importance of electrostatic factors in the intermolecular interaction, since the mutation will change a positively charged residue (His) into a neutral one (Asp)(at low pH).

In mutants with multiple substitutions, the interpretation of the results is more ambiguous. For the mutant Leu^{A13}+Gln^{A17}+Glu^{B10}+Gln^{B17}+des^{B1} with substitutions to more hydrophilic residues, the lag time was only slightly increased. The mutant Glu^{A15}+Asp^{A18}+Asp^{B3} with substitutions of amide groups to carboxyl groups formed fibrils with a significant longer lag time, indicating that the presence of the carboxyl groups inhibits the nucleation step in insulin fibril formation, as was also the case for the mutants Asp^{B25}, Asp^{B9}+Glu^{B27}, Glu^{B16}+Glu^{B27}, Glu^{A13}+Glu^{B10}, and Asp^{B10}. However, introducing a carboxyl group resulted in negligible effects on fibrillation lag times for the mutants, Glu^{B27}, Asp^{B28}, and Glu^{B1}+Glu^{B27}. Earlier fibrillation studies showed that insulin fibril formation is not dependent on the presence of carboxyl groups (*6*).

Interestingly, bovine insulin formed fibrils with a much shorter lag time at pH 7.4 than the corresponding human insulin, yet at pH 2 in the monomeric form, the lag times were similar. A part of this difference must reflect differences in the ease of dissociation at neutral pH. In the monomeric forms, the bovine protein had a similar lag time and a slightly faster elongation rate. In contrast, at pH 1.6, bovine insulin also had a much shorter lag time than human insulin. Bovine insulin differs from human insulin in positions A8, A10, and B30, and according to the insulin fibril model, these three residues are not involved in the interactions in the fibril (*7*). Since the mutant Val^{A10} forms fibrils with significantly longer lag times than both bovine and human insulin, it is concluded that Val^{A10} is not responsible for the faster fibril formation of bovine insulin. The B30 residue does not seem to be important either, since human and porcine insulin do not have significantly different tendencies to form fibrils, and the only difference between these two species is the B30 residue (*34*). Apparently, the substitution of Thr to Ala in position A8 in bovine insulin plays a significant role for the greater tendency of bovine insulin to form fibrils. Ala^{A8} is located on the surface of the monomer of bovine insulin, and it has been suggested that the presence of this hydrophobic residue instead of Thr in human (and porcine insulin) promotes the interaction of insulin with hydrophobic surfaces, which might lead to the greater fibrillation tendency of bovine insulin (*9*).

Thus, the observed fibrillation tendencies of the mutants do not support the proposed molecular interactions based on the model *(7)* for insulin fibrillation (which involves a relatively nativelike conformation, except for the terminal regions of the B-chain).

A New Model for Insulin Fibrillation. A likely alternative model for insulin fibrillation, in agreement with earlier proposed models (*35*, *10*), is one involving a partially unfolded intermediate conformation as the precursor of associated species on the pathway to fibrils, Scheme 1. In this model, the critical species leading to aggregation is the partially folded intermediate, which is derived from the monomer. Association of this intermediate to form soluble oligomers ultimately leads to the nucleus which then forms the initial fibrillar species. The nucleus is here depicted as consisting of 4 units of insulin, but it may be a higher number. An unfolding model for insulin has been suggested

Scheme 1

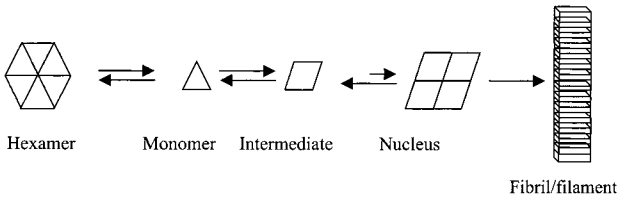

in which at least two partially folded intermediates are significantly populated (*30*). The first proposed intermediate is only slightly unfolded in the C-terminal segment of the B-chain. This is in agreement with the insulin fibril model based on DPI, as only minor unfolding of native insulin molecule is involved according to this model (*7*). The second and more stable intermediate retains only minimal secondary structure (*30*). Formation of a considerably unfolded intermediate supports the premise that insulin fibril formation involves substantial unfolding, which is also supported by other spectroscopic studies. Raman spectroscopy, small-angle X-ray diffraction studies, and FTIR spectroscopy on insulin fibrils all indicate a perturbed native structure with increased amount of β-sheet structure (*15*, *36*, *37*).

Examination of those mutants with the most significantly increased lag times, and most significantly decreased rates of elongations (in each case a factor of ≥ 2 relative to human zinc-free insulin at pH 2), reveals that there is a strong inverse correlation between the two effects, i.e., mutations which increased the lag time also decreased the rate of elongation, without exception. Since these results are for conditions where all the species are monomeric, the effects must reflect structural and thermodynamic properties of the specific mutants. If the initial conformation that associates on the fibrillation pathway is a partially folded intermediate that is in equilibrium with the monomer, but in rather low concentrations, the lag time would reflect both the population of the intermediate (and its rate of formation from the monomer) and its self-affinity. On the other hand, the rate of elongation would reflect the rate at which the intermediate is added to the growing fibril end. The simplest explanation to account for the similar effects of the mutations that both increase the lag time and decrease the rate of elongation is that the intermolecular interactions involved in the association of the putative partially folded intermediate to form the nucleus are very similar to those involved in the addition of a molecule of insulin to the growing fibril. This would suggest that it is also the partially folded intermediate conformation that adds to the growing fibril. That this is indeed the case is supported by the observation that seeding solutions of insulin with different insulin mutants leads to different rates of fibrillation, that the cognate fibrils always yielded the fastest fibrillation (data not shown), and that the addition of urea to insulin decreases the lag time simultaneously with an increase in the rate of elongation (*10*). Since most of the mutations leading to longer lag times involve substitutions leading to significantly more polar residues, it is likely that the aggregation-competent intermediate will have a lower hydrophobic driving force for self-association in these cases. The positions of these mutations are located all over the surface of the native conformation, and also scattered throughout the amino acid sequence, consistent with their effects being at the level of the nonnative intermediate.

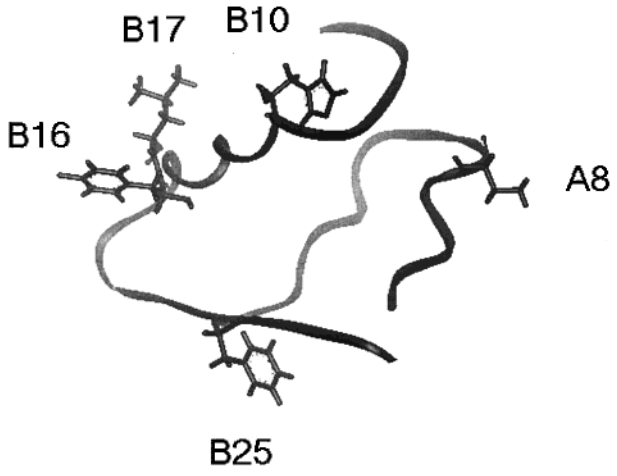

FIGURE 9: Structural cartoon of native insulin monomer (PDB ID 1BEN) showing the location of the two surfaces with residues whose mutation resulted in the largest increases in lag times in the kinetics of fibril formation.

The mutants with the largest increase in lag time relative to the wild-type under monomeric conditions were Asp^{B10} and Gln^{B17}, both of which involve mutations at the hexamer interface. The former involves conversion of His to Asp, and the latter involves substitution of Leu to Gln. Furthermore, mutation at the neighboring residue B16 of Tyr to Glu also resulted in significantly increased lag time under monomeric conditions. Based on the wild-type structure, His^{B10}, Tyr^{B16}, and Leu^{B17} would be quite solvent exposed in the native monomer and stick out from the helix in the native monomeric and dimeric conformation (Figure 9). The B10 residue is located two turns apart from the residues B16 and B17 on the helix. The longer lag times for these mutants suggest that His^{B10}, Tyr^{B16}, and Leu^{B17} may be involved in the intermolecular interfaces in the association of the putative partially folded intermediate.

Two additional sites in which mutations led to significant increases in lag time were B25 (Phe to Asp) and A8 (Thr to His). These two residues are located on the opposite side of the native conformation to B10, B16, and B17 (Figure 9). The conversion of the hydrophobic Phe into the polar Asp would result in a substantial change in the polarity in that region of the molecule. Since the adjacent residues to B25 are Phe^{B24} and Tyr^{B26}, the correspondence between the loss of the hydrophobic Phe^{B25} and the longer lag time suggests that this region of the B-chain may be important in the intermolecular association events that lead to fibril formation. Thr^{B26} and Val^{A10} are other substitutions resulting in increased lag times, further suggesting that regions of the insulin chain in the vicinity of A9 and B25 may also be important in the intermolecular association leading to fibrils. Thus, the intermolecular interactions in insulin fibrils seem to involve the residues B10, B16, and B17 from one molecule in contact with the residues, A8, B25, and possibly A10, B24, and B26, from another molecule. This is further supported by the fact that mutation of Thr^{A8} to the positively charged His increased the lag time at low pH. If the residues B10 and A8 are involved in the intermolecular association in the insulin fibrils, the mutation at A8 to His will result in repulsion between the two positively charged His, explaining the increase in the lag time for the mutant His^{A8}.

Thus, insulin fibril formation involves specific intermolecular interactions that are sensitive to variations in the primary structure. We propose that insulin fibril formation proceeds through the formation of a partially folded intermediate, and that two surfaces on opposite sides of the insulin monomer are involved in the intermolecular association of the intermediate to form the nucleus and fibrils. The increase in the lag time for fibril formation with mutations to more polar residues or changes in the charge reflects the critical role of both electrostatic and hydrophobic interactions in the association of the intermediate leading to formation of the critical nucleus.

ACKNOWLEDGMENT

We thank Ritu Khurana, Keith Oberg and Guy Dodson for useful discussions, and Ian Millett for assistance with the SAXS experiments. We thank Axel Wollmer for providing des-(B1,B2)-insulin. Small-angle X-ray scattering data were collected at Beam Line 4-2 at Stanford Synchrotron Radiation Laboratory (SSRL). SSRL is supported by the US Department of Energy, Office of Basic Energy Sciences, and in part by the National Institutes of Health, National Center for Research Resources, Biomedical Technology Program.

REFERENCES

1. Blundell, T. L., Dodson, G. G., Hodgkin, D. M., and Merola, D. (1972) *Adv. Protein Chem. 26*, 279−402.
2. Baker, E. N., Blundell, T. L., Cutfield, J. F., Cutfield, S. M., Dodson, E. J., Dodson, G. G., Hodgkin, D. M., Hubbard, R. E., Isaacs, N. W., Reynolds, C. D., Sakabe, K., Sakabe, N., and Vijayan, N. M. (1988) *Philos. Trans. R. Soc. 319*, 369−456.
3. Brange, J., Skelbaek-Pedersen, B., Langkjaer, L., Damgaard, U., Ege, H., Havelund, S., Heding, L. G., Jorgensen, K. H., Lykkeberg, J., Markussen, J., Pingel, M., and Rasmussen, E. (1987) *Galenics of insulin. The physicochemical and pharmaceutical aspects of insulin and insulin preparations*, Springer-Verlag, Berlin.
4. Bryant, C., Spencer, D. B., Miller, A., Bakaysa, D. L., McCune, K. S., Maple, S. R., Pekar, A. H., and Brems, D. N. (1993) *Biochemistry 32*, 8075−8082.
5. Waugh, D. F. (1946) *J. Am. Chem. Soc. 68*, 247−250.
6. Waugh, D. F., Wilhelmson, D. F., Commerford, S. L., and Sackler, M. L. (1953) *J. Am. Chem. Soc. 75*, 2592−2600.
7. Brange, J., Dodson, G. G., Edwards, D. J., Holden, P. H., and Whittingham, J. L. (1997) *Proteins 27*, 507−516.
8. Brange, J., Whittingham, J., Edwards, D., Youshang, Z., Wollmer, A., Brandenburg, D., Dodson, G., and Finch, J. (1997) *Curr. Sci. 72*, 470−476.
9. Brange, J., Andersen, L., Laursen, E. D., Meyn, G., and Rasmussen, E. (1997) *J. Pharm. Sci. 86*, 517−525.
10. Nielsen, L., Khurana, R., Coats, A., Frokjaer, S., Brange, J., Vyas, S., Uversky, V. N., and Fink, A. L. (2001) *Biochemistry 40*, 6036−6046.
11. Brange, J., Owens, D. R., Kang, S., and Volund, A. (1990) *Diabetes Care 13*, 923−954.
12. Weiss, M. A., Nguyen, D. T., Khait, I., Inouye, K., Frank, B. H., Beckage, M., O'Shea, E., Shoelson, S. E., Karplus, M., and Neuringer, L. J. (1989) *Biochemistry 28*, 9855−9873.
13. Hua, Q. X., and Weiss, M. A. (1991) *Biochemistry 30*, 5505−5515.
14. Brange, J., and Langkjaer, L. (1992) *Acta Pharm. Nord. 4*, 149−158.
15. Nielsen, L., Frokjaer, S., Carpenter, J. F., and Brange, J. (2001) *J. Pharm. Sci. 90*, 29−37.
16. Teplow, D. B. (1998) *Amyloid: Int. J. Exp. Clin. Invest. 5*, 121−142.
17. Jarrett, J. T., and Lansbury, P. T. (1993) *Cell 73*, 1055−1058.
18. Lomakin, A., Chung, D. S., Benedek, G. B., Kirschner, D. A., and Teplow, D. B. (1996) *Proc. Natl. Acad. Sci. U.S.A. 93*, 1125−1129.
19. Wood, S. J., Wypych, J., Steavenson, S., Louis, J. C., Citron, M., and Biere, A. L. (1999) *J. Biol. Chem. 274*, 19509−19512.
20. Levine, H. (1993) *Protein Sci. 2*, 404−410.
21. Porter, R. R. (1953) *Biochem. J. 53*, 320−328.
22. Gill, S. C., and Hippel, P. H. (1989) *Anal. Biochem. 182*, 319−326.
23. Waugh, D. F. (1948) *J. Am. Chem. Soc. 70*, 1850−1857.
24. Eftink, M. R., and Ghiron, C. A. (1981) *Anal. Biochem. 114*, 199−227.
25. Glatter, O., and Kratky, O. (1982) *Small-angle X-ray scattering*, Academic Press, New York.
26. Schmid, F. X. (1997) in *Protein Structure. A practical approach* (Creighton, T. E., Ed.) pp 261−297, IRL Press at Oxford University Press, Oxford.
27. Chen, Y. H., Yang, J. T., and Chau, K. H. (1974) *Biochemistry 13*, 3350−3359.
28. Sluzky, V., Tamada, J. A., Klibanov, A. M., and Langer, R. (1991) *Proc. Natl. Acad. Sci. U.S.A. 88*, 9377−9381.
29. Redondo, C., Damas, A. M., and Saraiva, M. J. (2000) *Biochem. J. 348*, 167−172.
30. Millican, R. L., and Brems, D. N. (1994) *Biochemistry 33*, 1116−1124.
31. Ludvigsen, S., Roy, M., Thogersen, H., and Kaarsholm, N. C. (1994) *Biochemistry 33*, 7998−8006.
32. Soto, C., Castano, E. M., Kumar, R. A., Beavis, R. C., and Frangione, B. (1995) *Neurosci. Lett. 200*, 105−108.
33. Porter, R. R. (1950) *Biochem. J. 46*, 304−307.
34. Brange, J., Havelund, S., Hommel, E., Sorensen, E., and Kuhl, C. (1986) *Diabetic Med. 3*, 532−536.
35. Brange, J., and Langkjaer, L. (1993) in *Stability and Characterization of Proteins and Peptide Drugs: Case Histories* (Wang, Y. J., and Pearlman, R., Eds.) pp 315−350, Plenum Press, New York.
36. Yu, N. T., Jo, B. H., Chang, R. C., and Huber, J. D. (1974) *Arch. Biochem. Biophys. 160*, 614−622.
37. Burke, M. J., and Rougvie, M. A. (1972) *Biochemistry 11*, 2435−2439.

BI0105983